

# Engineering Notes

## Safe Zone for Closely Spaced Parallel Approaches

Steven J. Landry\* and Alfred Lynam

*Purdue University, West Lafayette, Indiana 47907*

DOI: 10.2514/1.52567

### I. Introduction

THE predominant approach to managing safety for aircraft on closely spaced parallel approaches has been to detect and resolve (DAR) potential collisions caused by one aircraft unexpectedly turning toward the other (blundering) while remaining clear of the wake vortices of the other aircraft [1–3]. Other efforts have attempted to ensure that an escape maneuver is available, and alert just before the predetermined maneuver or range of maneuvers is no longer available [4,5].

In this Note, a method is introduced to structure the geometry of aircraft on approach to closely spaced parallel runways such that a predetermined amount of time is available to respond to an alert. That is, a zone for the trailing aircraft relative to the lead aircraft is computed such that the two aircraft cannot pass within 500 ft of one another within a prescribed period of time in the event of a blunder while also remaining clear of the wake vortices of the other aircraft.

This method is a different, and perhaps complementary, approach to DAR methods, in that it can be used to softly constrain the geometry of the problem. An alert can coincide with an aircraft leaving the safe zone, but that is not a necessary feature of the safe zone.

The Note first describes the relationship of the work to past research, introduces the problem, and then presents the method for determining the safe zone. Analysis of the safe zone for different geometries is then presented, showing that the safe zone is feasible and increases capacity over current operations.

In general, three major classes of approaches have been used to design alerting systems for closely spaced, parallel approach alerting and similar problems [6]. These approaches include monitoring for compliance, alerting based on noncompliance [1], monitoring for a future hazard state, and alerting based on some threshold such as, response time [4,7]. (The former can be thought of as answering the question: Given behavior of the aircraft in comparison to nominal behavior, should I alert? Whereas the latter answers the question: Given projected nominal positions of the aircraft, should I alert?) A third method monitors for availability of an escape maneuver and alerts just before escape maneuvers become unavailable [5]. There are also combinations of these methods that can be used. In addition, Yang and Kuchar [8] have recommended that alerting systems be designed to directly reflect the performance metrics associated with them, such as false alarm probability.

DAR methods are driven by a tradeoff between the time to resolve upon detection and the false alarm rate [8,9]. That is, when setting alert thresholds, one can choose either a low false alarm rate or a long

time to resolve, but the two cannot be set independently when uncertainty increases with increasing time before the event. (Such increasing uncertainty occurs in nearly every practical instance of alerting systems.)

For aircraft alerting systems, this tradeoff results in either a high false alarm rate, when pilots are given ample time to respond to an alert, or an extremely short time to respond, when the false alarm rate is required to be low. Low false alarm rates are desired, because human performance suffers when automation is unreliable [10–14]. Very short times to respond, although commonly assumed for alerting systems [15–17], may be unrealistic given the rare and unexpected nature of the alert. Recent work on this issue has suggested that a more realistic response time may be several tens of seconds [18], and experience with the traffic collision avoidance system indicates that pilots have not responded within the required response time in a majority of cases [16].

The work described in this Note is essentially a performance-based method, as promoted by Yang and Kuchar [8], where alert thresholds are set based on controlling some performance parameter but differ in two ways. First, the method can be used to identify relative risk rather than necessarily be used as a threshold for alerting. That is, such a system can be used in addition to, rather than instead of, a separate DAR-based alerting system. Second, the method controls for time to respond as the performance measure rather than a projection of false alarm rate.

The approach uses simple aircraft kinematic equations to determine an expression for the minimum time to a lateral separation of 500 ft between the centers of mass of the aircraft. [Five hundred feet is used, because collision is ambiguous with respect to the separation of the centers of mass, and 500 ft lateral separation corresponds to the definition of a near-midair collision (NMAC) by the U.S. Federal Aviation Administration (FAA).] The vertical domain is ignored due to large uncertainties in projections of vertical position; it is assumed that, in this approach domain, when one aircraft is blundering, the possibility of being close vertically is high.

The equations assume minimal limits on the possible blunders, but they also assume a simple blunder where the aircraft turns to an offset heading and remains on the heading for the remainder of the blunder. The solutions are also based on the current speed of the two involved aircraft and assume that no speed changes occur during the encounter.

Because of the short time over which the solutions need to be accurate, these assumptions are deemed sufficient, but the equations could be altered to account for more complex blunders. The effect of accounting for more complex blunders would be to make the equations more complex, incurring more time to find a solution. A cursory study of the need to include the rate of blunder heading rate change indicated its effect on the solutions was negligible.

The method is ensuring that a particular time to respond is available. This time, called the protection time, can be selected, but it is expected to be on the order of 30 s. As will be shown, this (approximate) amount of time results in a manageable range of allowable positions under most conditions while still allowing several tens of seconds for detection and resolution of blunders.

Equations describing the separation of the pair of aircraft are solved for the initial separation that yields a minimum separation of 500 ft within the protection time. The equations are a quadratic, resulting in a front and back of a danger zone, within which separations of 500 ft or less can be achieved in less than the protection time. Outside of the danger zone, the aircraft will require more than the protection time to get within 500 ft of one another. The back of the danger zone is therefore the front of a safe zone.

The back of the safe zone is neglected in this work. A procedure whereby the trailing aircraft is upwind would eliminate the need to

Received 27 September 2010; revision received 5 October 2010; accepted for publication 19 October 2010. Copyright © 2010 by Steven J. Landry. Published by the American Institute of Aeronautics and Astronautics, Inc., with permission. Copies of this Note may be made for personal or internal use, on condition that the copier pay the \$10.00 per-copy fee to the Copyright Clearance Center, Inc., 222 Rosewood Drive, Danvers, MA 01923; include the code 0731-5090/11 and \$10.00 in correspondence with the CCC.

\*Assistant Professor, School of Industrial Engineering, 315 North Grant Street. Member AIAA.

consider wake; extensions to downwind cases can be handled by predicting the position of the wake vortex and adjusting the protection time or by actively avoiding the wake [19]. Models for predicting the wake have been developed [20,21]. The focus of this work was on developing a method for determining the front of the safe zone, but the back of the wake is not considered to be an impediment to implementation, except that the lead aircraft cannot be allowed to cross in front of the trailing aircraft.

Safe zone information could be used in a number of ways. It is possible that the method could be used to identify positions of relative safety as guidance for current visual approaches to closely spaced parallel approaches without the need for any additional equipment. Another application would involve integrating an indication of the safe zone on the aircraft's primary or secondary flight instruments. In such a case, the safe zone could be used as an advisory system, indicating that very little time is available to respond to a lead aircraft blunder. Last, the safe zone could be used as a warning system, where leaving the safe zone requires an immediate escape maneuver. The flexibility of how one might apply the results of this method is seen as a significant advantage of the approach.

## II. Computation of Safe Zone

The geometry of aircraft on closely spaced parallel approach is shown in Fig. 1, and the reference frame is shown in Fig. 2. A lead aircraft is on approach to a runway, with a trailing aircraft on approach to a parallel runway for which the lateral separation is low (less than 4300 ft). The trailing aircraft must avoid two hazards: the wake vortices shed by the leading aircraft and the hazard associated with an unexpected blunder by the lead aircraft that poses a collision danger. The current range of positions that avoids these two hazards is referred to as the safe zone.

In this geometry, the trail aircraft would need to establish a speed equal to or greater than the lead to maximize capacity. (If the trail aircraft were slower, runway throughput would be lost due to the need to maintain minimum separation at the start of the approach, such that the separation at the runway would be greater than the minimum.)

Ideally, the trail aircraft would be placed such that under no reasonable blunder dynamics (turn rate and turn extent) could the lead aircraft collide with the trail aircraft. In addition, it should not be possible for the trail aircraft to interact with the wake vortices of the lead aircraft.

Therefore, the back of the safe zone is driven by the need to be in front of the position where the lead's wake will cross the trail's path. (This represents a significant departure from today's instrument approaches, where the aircraft is provided spacing to keep it behind the wake of the lead aircraft.) While more sophisticated methods to calculate wake vortex dynamics exist [20], for simplicity, the wake is modeled as crossing at the speed of crosswind. The back of the safe zone is then given by

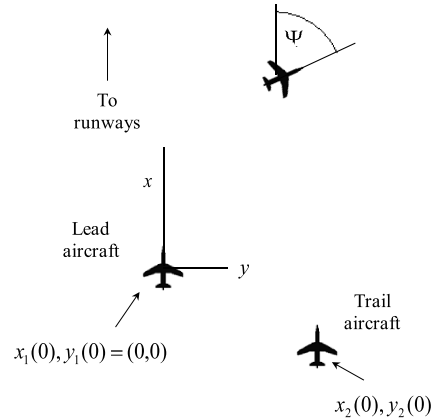


Fig. 2 Reference frame.

$$x_{\text{wake}} = v_2 \left( \frac{y_2}{v_{x\text{wind}}} \right) \quad (1)$$

Again, the back of the safe zone can be ignored if the crosswind component in the direction of the trail aircraft is zero. In that case, the wake will not reach the trailing aircraft's flight path unless the lead approaches the trailing aircraft's flight path.

The front of the safe zone is driven by the need to not be in a position such that a blundering lead aircraft will cause a collision. That is, the trail aircraft, if the lead turns toward its flight path (blunders), should not be able to pass within a close distance of the lead if the trail aircraft continues along the final approach course. (Close distance is defined in this work as within 500 ft, which is the FAA definition of a NMAC.)

Using point-mass kinematics, simple equations can be derived for the future positions of both aircraft, assuming the trail remains on the final approach course and the lead turns to a new heading and continues along a new course. An expression for the separation of the aircraft through time after the blunder turn is completed is then given by the square root of the squared differences of the  $x$  and  $y$  positions.

The restriction on the equations being valid only after the blunder turn is completed is believed to lead to no loss of generality. As will be seen, the front of the safe zone will be driven by small values of blunder turn extent and high values of blunder turn rate.

Of course, without assuming limitations on the blunder dynamics or time to collide, such an assurance cannot be made. For example, a sufficiently tight turn radius and a  $180^\circ$  turn extent would result in the lead turning directly back on the trail aircraft, which would mean that there is no safe zone. Restrictions on the blunder dynamics will be discussed later in the Note.

Unlike DAR methods where one is concerned with the fastest reasonable blunder dynamics, in this case, slow blunder dynamics will drive the solutions. That is, if the trail has some overtake on the

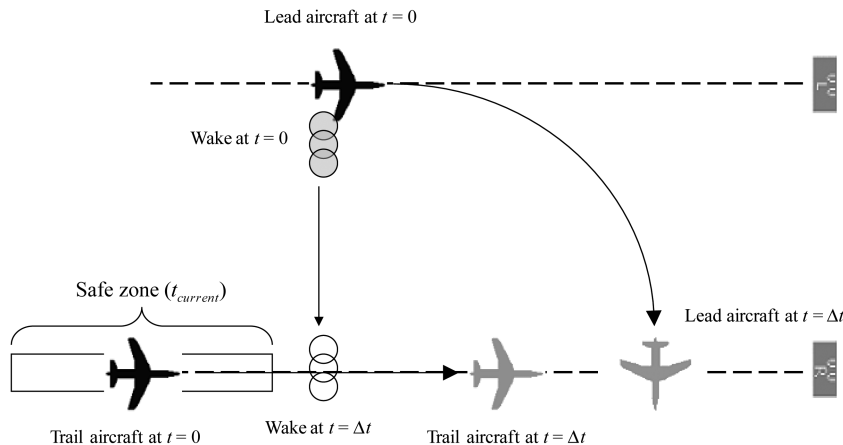


Fig. 1 Closely spaced parallel approach geometry.

lead, the longer the time the blundering lead aircraft takes to reach the trail's path, the longer the trail's overtake has to affect the separation and the further in trail the trail aircraft needs to be.

The separation between the aircraft is given by Eq. (2):

$$D = \sqrt{[x_1(t) - x_2(t)]^2 + [y_1(t) - y_2(t)]^2} \quad (2)$$

If we consider a simple blunder where the lead aircraft turns (blunders) to some heading and then continues along that flight path, then the equations of the  $x$  and  $y$  coordinates after the blunder turn are given by (3)

$$\begin{aligned} x_1(t) &= \int_0^{T_{\text{turn}}} v_1 \cos(\dot{\Psi}\tau) d\tau + v_1(t - T_{\text{turn}}) \cos \Psi \\ y_1(t) &= \int_0^{T_{\text{turn}}} v_1 \sin(\dot{\Psi}\tau) d\tau + v_1(t - T_{\text{turn}}) \sin \Psi \\ x_2(t) &= x_2(0) + v_2 t, \quad y_2(t) = y_2(0) \end{aligned} \quad (3)$$

where  $x_2(0)$  is the initial trail aircraft longitudinal position (relative to lead),  $y_2(0)$  is the initial lead aircraft lateral position (relative to lead),  $v_1$  is the speed of the lead aircraft,  $v_2$  is the speed of the trail aircraft,  $\Psi$  is the blunder heading change, and  $\dot{\Psi}$  is the blunder heading change rate.

It is assumed that we know the positions of the two aircraft and their speeds but that we do not know what blunder will be committed. Integrating these equations then yields the following:

$$\begin{aligned} x_1(t) &= \frac{v_1}{\dot{\Psi}} \sin \Psi + v_1(t - T_{\text{turn}}) \cos \Psi \\ y_1(t) &= \frac{v_1}{\dot{\Psi}} (1 - \cos \Psi) + v_1(t - T_{\text{turn}}) \sin \Psi \\ x_2(t) &= x_2(0) + v_2 t, \quad y_2(t) = y_2(0) \\ D^2 &= x_2^2 + K_1 + K_2 t^2 + K_3 + K_4 t^2 \end{aligned} \quad (4)$$

where

$$\begin{aligned} x_{\text{turn}} &= \frac{v_1}{\dot{\Psi}} \sin \Psi, \quad y_{\text{turn}} = \frac{v_1}{\dot{\Psi}} - \frac{v_1}{\dot{\Psi}} \cos \Psi \\ K_1 &= x_{\text{turn}}^2 - v_1 \frac{\Psi}{\dot{\Psi}} \cos \Psi, \quad K_2 = v_1 \cos \Psi - v_2 \\ K_3 &= y_{\text{turn}}^2 - y_2(0) - v_1 \frac{\Psi}{\dot{\Psi}} \sin \Psi, \quad K_4 = v_1 \sin \Psi \end{aligned}$$

The position in which we are interested is the minimum root of Eq. (5), where  $t = t_{\text{prot}}$  such that the separation is equal to  $500^2$ . The term  $t_{\text{prot}}$  is the protection time, which is the amount of time for which protection from a blundering lead aircraft is provided. Since the slow blunder dynamics will drive the solution, if  $t_{\text{prot}}$  is not set, the required distance in trail will need to be quite large to prevent slow blunders that take a very long time to induce a collision risk. That is, the two solutions to the quadratic with respect to  $x_2(0)$  resulting in a separation of  $500^2$  at  $t_{\text{prot}}$  will be the safe zone; the quadratic is shown in Eq. (6):

$$\begin{aligned} x_2^2 - 2(K_1 + K_1 t_{\text{prot}})x_2 + K_2^2 + K_4^2 t_{\text{prot}}^2 + 2K_1 K_2 \\ + K_3 K_4 t_{\text{prot}} + K_1^2 + K_3^2 - 500^2 = 0 \end{aligned} \quad (6)$$

Equation (6) can be solved using the quadratic equation, yielding two expressions for  $x_2(0)$ , which are the front and back of the danger zone. Inside of these two values, the minimum separation drops below 500 ft within  $t_{\text{prot}}$ . Outside of them, the separation does not reach 500 ft within  $t_{\text{prot}}$ . The front of the danger zone is of no interest.

Without constraints, the blunders that cause the separation to drop below 500 ft could be unreasonable, such as assuming an infeasible rate of heading change. Constraining blunder heading change limits the turn rate of the lead blundering aircraft. We therefore constrain the blunder heading change. To be conservative, this rate was set to  $12^\circ/\text{s}$ . Increasing this has little effect on the solutions, as will be

shown, but decreasing it significantly affects the solution. Therefore, we are interested in the minimum root of Eq. (6), with the constraint that

$$\dot{\Psi} < \frac{\pi}{12}$$

The solution can be obtained iteratively using a nonlinear solver. The problem for the solver is as follows (the negative root is taken so as to yield the back of the danger zone rather than the front):

Minimize

$$x_2(0) = \frac{-b - \sqrt{b^2 - 4ac}}{2a} \quad (7)$$

where

$$a = 1, \quad b = -2(K_1 + K_5 t_{\text{prot}}),$$

$$c = K_2^2 + K_4^2 t_{\text{prot}}^2 + 2K_1 K_2 + K_3 K_4 t_{\text{prot}} + K_1^2 + K_3^2 - 500^2$$

such that

$$b^2 - 4ac > 0, \quad \dot{\Psi} < \frac{\pi}{12}$$

The solution will yield a distance in trail such that no blunder of less than  $12^\circ/\text{s}$  will result in a NMAC within  $t_{\text{prot}}$ . The solution will also produce the worst-case blunder heading change; that is, the blunder heading that produces the maximum required distance in trail will result from solving the equation.

Equation (7) can then be solved for various input parameters ( $y_2(0)$ ,  $v_1$ ,  $v_2$ ), each of which can be obtained in real time if the aircraft are using either Mode S or ADS-B systems. It may also be possible to obtain these values from the traffic collision avoidance system. (Otherwise, they can be set to the worst-case values, assuming adherence to the procedure, although that has implications for the procedures used by the pilots.)

It is shown, therefore, that such a region is calculable. What is now of interest are the dynamics of the safe zone, whether there is a practical zone for operationally meaningful geometries, and whether that zone significantly reduces capacity under those conditions.

To test this, the safe zone was calculated for a number of conditions. The safe zone was calculated for  $t_{\text{prot}}$  values of 30, 45, and 60 s and for lateral separations of 750 to 3000 ft. Lead and trail speed differences of 5 to 60 kt were also considered.

### III. Results and Discussion

The equations were solved using a nonlinear solver. The solver's tolerance was set to 5%, with a convergence value of 0.001. Solutions had a required precision of 0.000001. Solutions for a single problem were calculated within 1 s, although no attempt was made to control the speed of the algorithm, since it is not yet clear the solutions would need to be solved dynamically in real time.

#### A. Safe Zone Dynamics

First, as expected, it was found that the solutions for the front of the safe zone were driven by relatively slow blunders as compared with those considered by DAR algorithms. The solutions resulted from the maximum blunder turn rate of  $12^\circ/\text{s}$ . As shown in the example in Fig. 3, the worst-case blunder turns extents (i.e., those that produce the maximum value of the minimum allowed distance in trail) are low at low values of lateral separation. Because of the constraint that the minimum separation of 500 ft be obtained within the protection time, this increases as the lateral separation increases. The worst-case blunders are constant for a given lead speed, since the lead's lateral and vertical distances travelled during the blunder would be the same; the trail speed only changes the required distance in trail.

The front of the safe zone solutions were calculated for a range of  $t_{\text{prot}}$ , speed differences, and lateral separations. An example of the output is shown in Fig. 4. The minimum allowed distance in trail increases with greater lateral separation and greater protection time.

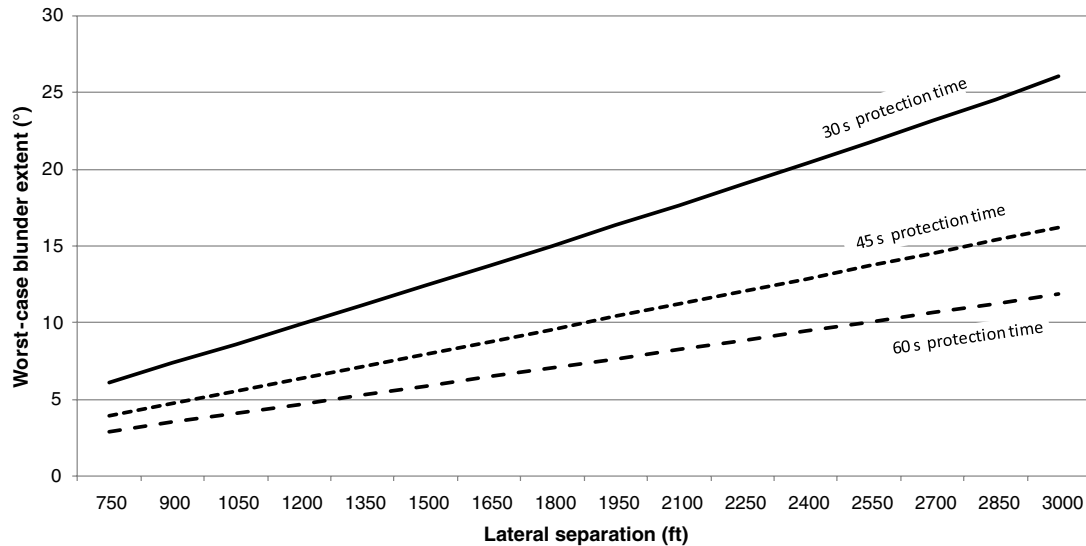


Fig. 3 Worst-case blunder turn extent vs lateral separation for lead speed of 150 kt.

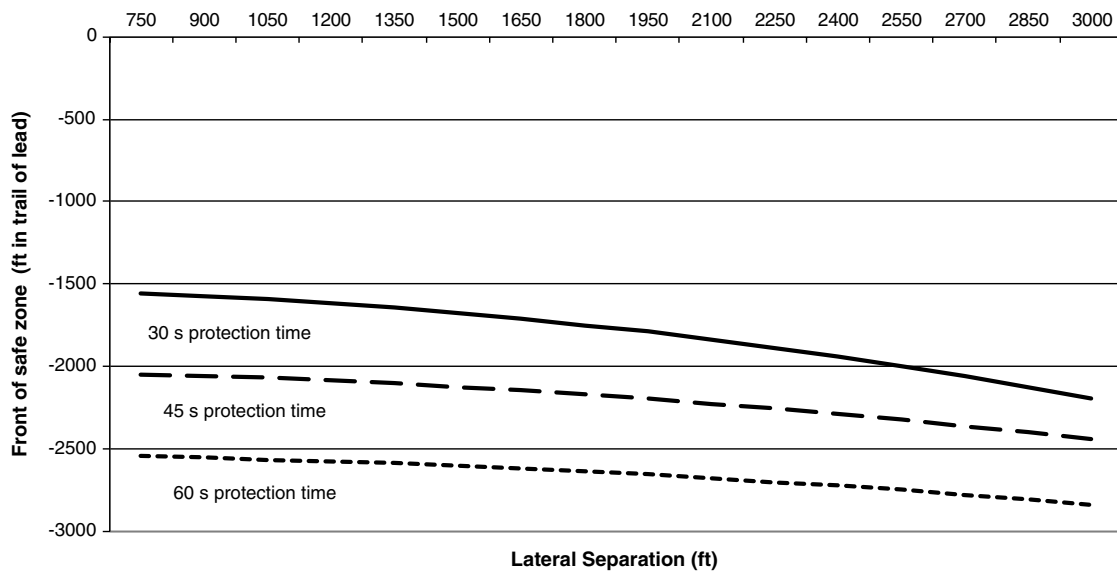


Fig. 4 Front of the safe zone vs lateral separation for a lead speed of 150 kt and a trail speed of 170 kt.

However, the range of distances is reasonable for the cases shown in Fig. 4: within 0.5 nautical miles of the lead aircraft.

The solutions were checked against numerical simulation of the kinematic trajectories. Plots of the trajectories for several of the preceding cases are shown in Figs. 5a–5c. In Fig. 5, the endpoints of the trajectories are the points where separation drops below 500 ft at  $t_{\text{prot}}$ . The trailing aircraft is required to be further in trail for larger lateral separations, and the lead aircraft must have a larger blunder extent.

In general, the front of the safe zone was influenced by speed differences but not substantially by the lead aircraft speed given the same speed difference. For  $\pm 20$  kt lead speed, the front of the safe zone changed by no more than 5%, with larger changes occurring at the greater lateral separations and less than 1% differences at 750 ft lateral separation. Larger speed differences resulted in a front of safe zone that is farther in trail of the lead. Figure 6 shows the effect of speed differences on the front of the safe zone.

## B. Impact on Capacity

The front of the safe zone varies mainly with the lateral separation and speed difference between the lead and trail, with very little variation by lead speed when the speed difference is kept constant.

This distance in trail can be compared with current operations to estimate the impact on throughput.

Under current operations, aircraft on parallel runways that are more than 4300 ft apart are treated independently. Under visual conditions, this independence in theory is true for any runway separation, although typically, some stagger (slant range separation between the aircraft) is necessary to adhere to the “remain in visual contact with the other aircraft” requirement. Inside of 4300 ft, but greater than 2500 ft, a 1.5 n mile stagger must be used. Inside of 2500 ft, the runways are considered dependent, and standard wake vortex separation of at least 2.5 n mile longitudinally must be provided.

At some airports, a high-update radar and monitoring system called the precision runway monitoring (PRM) system is installed. This allows the assumption of independence of the runways to be extended to runways of separations of 3400 ft or more. PRM provides no benefit for runways that are separated by less than 3400 ft.

In this work, we can compute a rough estimate of throughput impact by comparing the longitudinal separation requirements of the various methods. Forty knots of speed difference provides a highly restrictive safe zone (farther in trail than safe zones with smaller speed differences). A comparison for lateral separations of 750 to 3000 ft is shown in Fig. 5. Clearly, even if one adds a small buffer

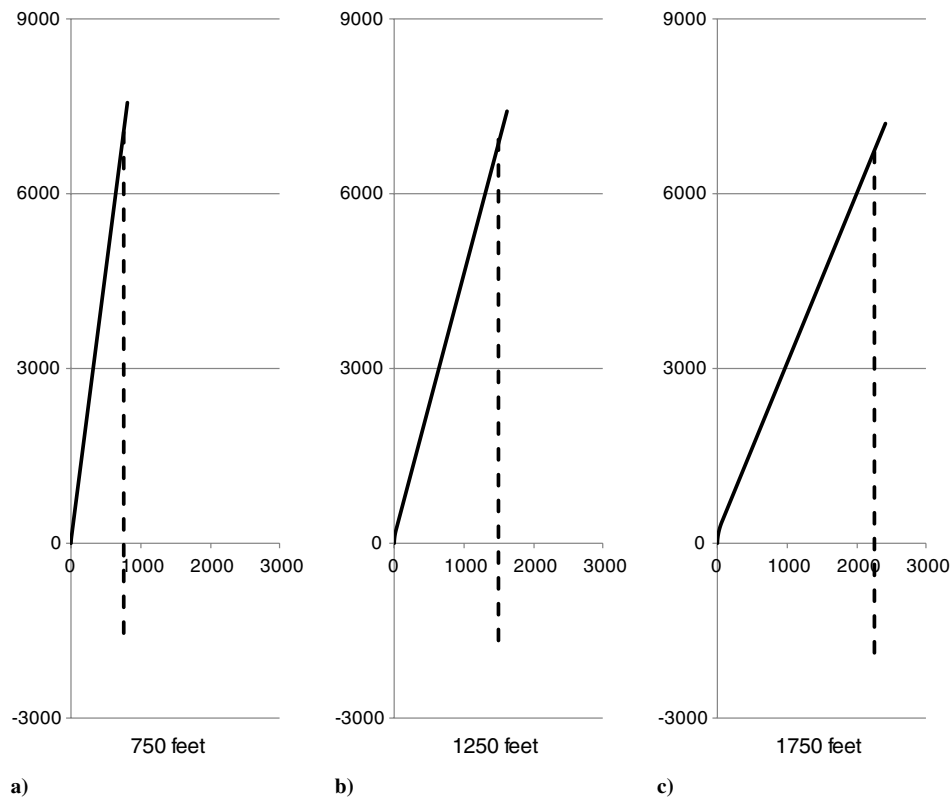


Fig. 5 Simulated kinematic trajectories for worst-case blunders.

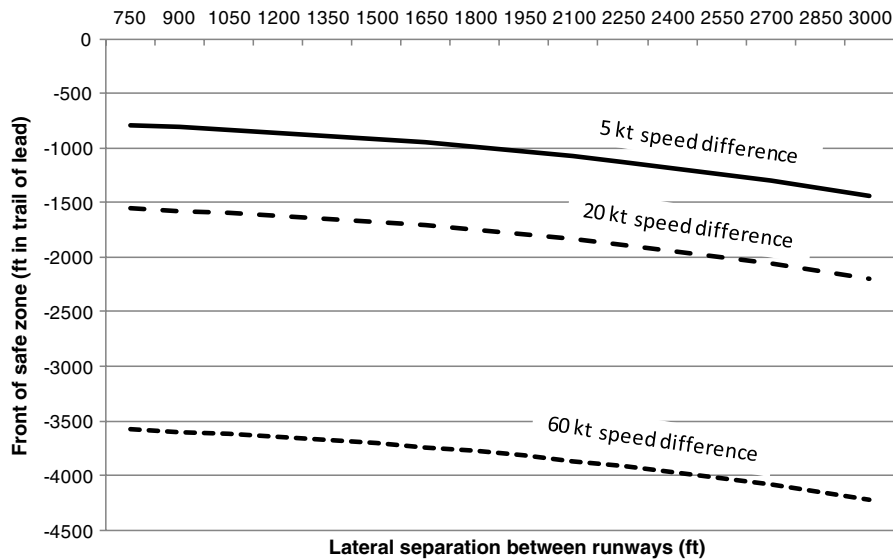


Fig. 6 Front of safe zone vs lateral separation and speed difference.

Table 1 Separation requirement comparison between standard operations and safe zone

Lateral separation	Standard operations	CSPA <sup>a</sup> with 20 kt speed difference		
		$T_{\text{prot}} = 30 \text{ s}$	$T_{\text{prot}} = 45 \text{ s}$	$T_{\text{prot}} = 60 \text{ s}$
750	>2.5	0.26	0.34	0.42
1000	>2.5	0.26	0.34	0.42
1250	>2.5	0.26	0.34	0.42
1500	>2.5	0.27	0.34	0.42
1750	>2.5	0.27	0.35	0.43
2000	>2.5	0.28	0.35	0.43
2250	>2.5	0.28	0.35	0.43
2500	1.44	0.29	0.36	0.43
2750	1.43	0.29	0.36	0.44
3000	1.42	0.30	0.37	0.44

<sup>a</sup>CSPA denotes closely spaced parallel approach.

behind the front of the safe zone, throughput improvements over standard operations should be substantial, since the separation requirements are substantially less than during standard operations (see Table 1).

#### IV. Conclusions

A safe zone can be computed that provides protection against blunders for a predetermined period of time. This safe zone has a reasonable width under most conditions, and adhering to the safe zone should improve capacity over current methods for closely spaced parallel approaches.

The safe zone is influenced by the time needed for responding to an alert, the speed difference between the two aircraft, the lateral separation between the paths of the aircraft, and the crosswind speed. Greater speed differences, larger speed differences, and wider lateral separations result in more distant in-trail separations. Higher crosswind speeds reduce the width of the safe zone. A practical safe zone exists up to approximately 40 kt difference in speed and 40 kt crosswind for runways, down to 750 ft lateral separation.

Implementing the safe zone, while reducing capacity when compared with independent operations, has a significant improvement over current operations. The guidance can be applied to current visual approaches, without the addition of any instrumentation, to improve the safety of those approaches without substantially impacting capacity. If a depiction is provided on a primary or secondary flight instrument, the safe zone may allow for closely spaced parallel approaches in instrument conditions to runways down to 750 ft lateral separation.

#### Acknowledgments

Thanks goes to the support of technical monitors Vern Battiste and Gene Wong, who supported this work under grant NAG-2-1314. The authors would like to thank the guidance of Amy Pritchett in the formulation of this problem and to thank Julie A. Jacko for her guidance on understanding the application of this problem.

#### References

- [1] Shank, E. M., and Hollister, K. M., "Precision Runway Monitor," *Lincoln Laboratory Journal*, Vol. 7, No. 2, 1994, pp. 329–353.
- [2] Prandini, M., Hu, J., Lygeros, J., and Sastry, S., "A Probabilistic Approach to Aircraft Conflict Detection," *IEEE Transactions on Intelligent Transportation Systems*, Vol. 1, No. 4, 2000, pp. 199–220. doi:10.1109/6979.898224
- [3] Abbott, T., and Elliott, D., "Simulator Evaluation of Airborne Information for Lateral Spacing (Ails) Concept," NASA, TP 2001-210665, 2001.
- [4] Kuchar, J. K., and Carpenter, B. D., "Airborne Collision Alerting Logic for Closely Spaced Parallel Approach," *Air Traffic Control Quarterly*, Vol. 5, No. 2, 1997, pp. 111–127.
- [5] Teo, R., and Tomlin, C. J., "Computing Canger Zones for Provably Safe Closely Spaced Parallel Approaches," *Journal of Guidance, Control, and Dynamics*, Vol. 26, No. 3, 2003, pp. 434–443. doi:10.2514/2.5081
- [6] Winder, L. F., and Kuchar, J. K., "Generalized Philosophy of Alerting with Applications to Parallel Approach Collision Prevention," AIAA Guidance, Navigation, and Control Conference, Montreal, Canada, AIAA, Paper 2001-4052, 2001.
- [7] Hu, J., Prandini, M., and Sastry, S., "Optimal Coordinated Maneuvers for Three-Dimensional Aircraft Conflict Resolution," *Journal of Guidance, Control, and Dynamics*, Vol. 25, No. 5, 2002, pp. 888–900. doi:10.2514/2.4982
- [8] Yang, L. C., and Kuchar, J. K., "Performance Metric Alerting: A New Design Approach for Complex Alerting Problems," *IEEE Transactions on Systems, Man and Cybernetics, Part A: Systems and Humans*, Vol. 32, No. 1, 2002, pp. 123–134. doi:10.1109/3468.995534
- [9] Kuchar, J. K., and Yang, L. C., "A Review of Conflict Detection and Resolution Modeling Methods," *IEEE Transactions on Intelligent Transportation Systems*, Vol. 1, No. 4, 2000, pp. 179–189. doi:10.1109/6979.898217
- [10] Thomas, L. C., and Rantanen, E. M., "Human Factors Issues in Implementation of Advanced Aviation Technologies: A Case of False Alerts and Cockpit Displays of Traffic Information," *Theoretical Issues in Ergonomics Science*, Vol. 7, No. 5, 2006, pp. 501–523. doi:10.1080/14639220500090083
- [11] Wickens, C. D., and Colcombe, A., "Dual-Task Performance Consequences of Imperfect Alerting Associated With a Cockpit Display of Traffic Information," *Human Factors*, Vol. 49, No. 5, 2007, p. 839. doi:10.1518/001872007X230217
- [12] Bliss, J. P., and Dunn, M. C., "Behavioural Implications of Alarm Mistrust as a Function of Task Workload," *Ergonomics*, Vol. 43, No. 9, 2000, pp. 1283–1300. doi:10.1080/001401300421743
- [13] Stanton, N. A., and Baber, C., "Modelling of Human Alarm Handling Response Times: A Case Study of the Ladbroke Grove Rail Accident in the UK," *Ergonomics*, Vol. 51, No. 4, 2008, pp. 423–440. doi:10.1080/00140130701695419
- [14] Parasuraman, R., and Riley, V., "Humans and Automation: Use, Misuse, Disuse, Abuse," *Human Factors*, Vol. 39, No. 2, 1997, pp. 230–253. doi:10.1518/001872097778543886
- [15] Winder, L. F., and Kuchar, J. K., "Evaluation of Collision Avoidance Maneuvers for Parallel Approach," *Journal of Guidance, Control, and Dynamics*, Vol. 22, No. 6, 1999, pp. 801–807. doi:10.2514/2.4481
- [16] Kuchar, J. K., and Drumm, A. C., "The Traffic Alert and Collision Avoidance System," *Lincoln Laboratory Journal*, Vol. 16, No. 2, 2007, pp. 277–296.
- [17] Abbott, T. S., "Flight Test Evaluation of the Airborne Information for Lateral Spacing (Ails) Concept," NASA, TM 2002-211639, 2002.
- [18] Ennis, R. L., and Zhao, Y. J., "A Formal Approach to Analysis of Aircraft Protected Zone," *Air Traffic Control Quarterly*, Vol. 12, No. 1, 2004, pp. 75–102.
- [19] Hardy, G. H., and Lewis, E. K., "Cockpit Display of Traffic and Wake Information for Closely Spaced Parallel Approaches," Guidance, Navigation, and Control Conference, Providence, RI, AIAA Paper 2004-5106, 2004.
- [20] Rossow, V., "Vortex-Free Flight Corridors for Aircraft Executing Compressed Landing Operations," *Journal of Aircraft*, Vol. 43, No. 5, 2006, pp. 1424–1428. doi:10.2514/1.21614
- [21] Shortle, J., and Jeddi, B., "Using Multilateration Data in Probabilistic Analysis of Wake Vortex Hazards for Landing Aircraft," *Transportation Research Record: Journal of the Transportation Research Board*, Vol. 2007, No. 1, 2007, pp. 90–96. doi:10.3141/2007-11